

# Nonlinear decay of the inflaton: the onset of turbulence and thermalization

H P de Oliveira<sup>1</sup> and I Damião Soares<sup>2</sup>

<sup>1</sup> Universidade do Estado do Rio de Janeiro, Instituto de Física—Departamento de Física Teórica, CEP 20550-013 Rio de Janeiro, RJ, Brazil

<sup>2</sup> Centro Brasileiro de Pesquisas Físicas, Rua Dr Xavier Sigaud, 150, CEP 22290-180 Rio de Janeiro, RJ, Brazil

E-mail: [oliveira@dft.if.uerj.br](mailto:oliveira@dft.if.uerj.br) and [ivano@cbpf.br](mailto:ivano@cbpf.br)

Received 26 September 2005

Accepted 12 July 2006

Published 4 August 2006

Online at [stacks.iop.org/JCAP/2006/i=08/a=002](http://stacks.iop.org/JCAP/2006/i=08/a=002)

doi:10.1088/1475-7516/2006/08/002

**Abstract.** We study the nonlinear decay of the inflaton field with quartic potential,  $V(\phi) = \frac{1}{4}\lambda\phi^4$ , using the Galerkin projection method that provides a natural mode decomposition of the field with the modal coefficients having the dynamics of a set of nonlinear coupled harmonic oscillators. Three distinct phases are definitely characterized according to the role of the nonlinear couplings in the dynamics, starting from the linear regime of parametric resonance towards a final turbulent phase dominated by the nonlinear effects and connected to the chaotic behaviour of all modes, when the state of thermalization is accomplished. Two features of the turbulent stage are displayed: first, an effective mechanism of transfer of energy among the homogeneous modes and all other modes, initially resonant or not; second, the distribution of energy versus the modal wavenumber, characterizing the energy distribution per scale, which shows two distinct decoupled components. One of the components, connected to the energy distribution in small scales, has a Maxwell–Boltzmann form in thermal equilibrium with temperature  $T_R \simeq 10^2 \lambda M_{\text{Pl}}$ .

**Keywords:** inflation, physics of the early universe

---

**Contents**

<b>1. Introduction</b>	<b>2</b>
<b>2. The model: basic equations and implementation of the Galerkin method</b>	<b>3</b>
<b>3. Numerical results</b>	<b>6</b>
<b>4. The turbulent regime</b>	<b>8</b>
<b>5. Conclusions</b>	<b>13</b>
<b>Acknowledgments</b>	<b>14</b>
<b>References</b>	<b>14</b>

---

**1. Introduction**

In the realm of inflationary cosmology, the process of reheating plays a crucial role in the transition of the Universe from the inflationary phase into the radiation dominated phase, and in the creation of almost all matter constituting the present Universe. This process begins at the end of inflation with a stage of parametric resonance when the energy is rapidly transferred from the inflaton field into other matter fields, leading to particle production and inflaton decay, far away from thermal equilibrium [1]–[3], [5].

The main object of this paper will be to describe the nonlinear decay of the inflaton field in the theory  $\frac{1}{4}\lambda\phi^4$  after inflation. For this we shall use the Galerkin projection method that is largely applied in problems of fluid mechanics and turbulence [6]. The Galerkin method constitutes a powerful method for dealing with nonlinear problems described by any type of differential equation, and whose main aspect is to approximate a given partial differential equation by a finite set of coupled ordinary differential equations. In the realm of the problem under consideration, the Galerkin method naturally provides a mode decomposition of the fields (that is the basics of a QFT treatment of the problem) and gives the dynamical equations of the modal coefficients. This allows us to approach the problem from a dynamical system perspective, and the general dynamics of the inflaton field with its fluctuations during preheating can be understood as a set of nonlinear coupled harmonic oscillators, where the linearized equations account for the preheating phase in which parametric resonance takes place. As the higher mode oscillations are amplified, the nonlinear coupling begins to play a crucial role in the dynamics, restructuring the resonance towards a final stage of *thermalization*. The method allows us to follow the dynamics in the full nonlinear regime and in the long term, including the effects of backreaction and rescattering, that will be responsible for dynamically restructuring the resonance. Furthermore, the dynamical evolution of each mode can be followed and the chaotic behaviour of all modes, resonant or not, is established in a long term regime leading to a final *thermalization* of the produced particles. A picture of thermalization emerges as due to the development of a full turbulent stage connected to the chaotic behaviour of all modes.

These dynamical mechanisms were first approached in several fundamental papers [2, 3] in which the background was assumed to be unperturbed. Basically, by integrating numerically the field equations on the lattice [4], Klebnikov and Tkachev found several interesting nonlinear effects such as the set-up of parametric resonance in the initial stages of reheating, how the resonance can be terminated by the backreaction of produced particles, and a stage of the inflaton decay when the resonant peaks in the power spectrum begin to interact and smear out, in a process denoted by the authors as semiclassical thermalization. In some other papers the metric perturbations were included [8]–[10].

This paper is organized as follows. In section 2 the basic equations of the model are presented, along with the steps necessary for the implementation of the Galerkin method that culminate with the derivation of the dynamical system. In section 3 the numerical results obtained from the integration of the dynamical system are discussed. By keeping track of the full evolution of the homogeneous inflaton field, and of the resonant and nonresonant modes, we were able to envisage the presence of three distinct phases of the dynamics towards the thermalization, as a generic feature of the system. Accordingly, we have called them the linear, quasilinear and turbulent phases, inspired by the transition from the laminar to the turbulent regime found in fluid mechanics. In our approach the onset of turbulence will be of crucial importance for the transfer of energy among the modes, and therefore in the establishment of *thermalization*. We have also derived the energy spectrum of the inflaton field versus the wavenumber in the turbulent phase, making explicit this mechanism of energy transfer. For numerical simplicity we first perform the integration in a two dimensional spatial domain. However, with view to reliable results of genuine cosmological interest, the numerical calculations leading to an evaluation of the reheating temperature were performed in three dimensions. Also some of the figures of the text, generated from calculations in two dimensions, are obtained again in three dimensional calculations and shown to be qualitatively analogous. Finally, our conclusions are given in section 4.

## 2. The model: basic equations and implementation of the Galerkin method

The basic equation of our problem is the evolution of the inflaton field  $\phi(\mathbf{x}, t)$  with the potential  $V(\phi) = \frac{1}{4}\lambda\phi^4$ , in a spatially flat Friedmann–Robertson–Walker universe [1, 2]. Using the conformal time  $\tau$  defined by  $a(\tau) d\tau = \sqrt{\lambda}\phi_0(0)a(0) dt$ , the conformal field  $\varphi = \phi a(\tau)/\phi_0(0)a(0)$  and spatial coordinates  $\mathbf{x} \rightarrow \sqrt{\lambda}\phi_0(0)a(0)\mathbf{x}$ , it assumes the form

$$\varphi'' - \nabla^2\varphi - \frac{a''}{a}\varphi + \varphi^3 = 0 \quad (1)$$

where a prime stands for the derivative with respect to  $\tau$  and  $\phi_0(0)$  is the homogeneous component of the inflaton field at  $t = \tau = 0$ . At the end of inflation the inflaton field undergoes the phase of coherent oscillations. It can be shown that the effective energy–momentum tensor of the inflaton in the theory  $\frac{1}{4}\lambda\phi^4$  averaged over several oscillations is traceless [11], implying  $a(\tau) \sim \tau$ , and allowing us to set  $a'' = 0$  in equation (1).

In order to simplify our procedure, the integration of equation (1) will be first performed in a two dimensional square box  $\mathcal{D}$  of size  $L$  with periodic boundary conditions. The orthogonal functions that automatically satisfy these boundary conditions are

$\psi_{\mathbf{k}} = \exp((2\pi i/L) \mathbf{k} \cdot \mathbf{x})$ , where  $\mathbf{k} = (l, m)$  is the co-moving momentum (wavenumber vector), so that the Galerkin decomposition is

$$\varphi(\mathbf{x}, t) = \sum_{l=-N}^N \sum_{m=-N}^N a_{lm}(\tau) \psi_{lm}(x, y), \quad (2)$$

where  $N$  is the order of truncation to be chosen and  $\mathbf{x} = (x, y)$ . For each  $N$  there are  $(N+1)(N+2)/2$  distinct moduli of the wavenumber vectors  $\mathbf{k}$ , the latter corresponding to a large number of independent modes with the same moduli. The basis functions are orthogonal with respect to the inner product defined by  $\langle \psi_{\mathbf{k}}, \psi_{\mathbf{l}} \rangle = \int_{\mathcal{D}} \psi_{\mathbf{k}} \psi_{\mathbf{l}}^* d^2\mathbf{x} = L^2 \delta_{\mathbf{k}\mathbf{l}}$ . Not all modal coefficients  $a_{\mathbf{k}}(\tau)$  are independent, since by imposing the scalar field to be real, we arrive at  $a_{\mathbf{k}}^*(\tau) = a_{-\mathbf{k}}(\tau)$ , or equivalently  $a_{lm}^* = a_{-l-m}$ .

The next step of the Galerkin procedure is to insert the decomposition (2) into (1), the resulting equation then being projected into each  $\mathbf{k}$ th mode  $\psi_{\mathbf{k}}(\mathbf{x})$ . As a result, we obtain a set of equations for  $a_{\mathbf{k}}(\tau)$  given by

$$a_{\mathbf{k}}''(\tau) + \omega_{\mathbf{k}}^2 a_{\mathbf{k}}(\tau) + \sum_{\mathbf{n}, \mathbf{l}} a_{\mathbf{n}}(\tau) a_{\mathbf{l}}(\tau) a_{\mathbf{k}-\mathbf{n}-\mathbf{l}}(\tau) = 0, \quad (3)$$

where  $\omega_{\mathbf{k}}^2 = (4\pi^2/L^2) \mathbf{k}^2$ . A further decomposition of the modal coefficients into their real and imaginary parts is necessary, or  $a_{\mathbf{k}}(\tau) = \alpha_{\mathbf{k}}(\tau) + i\beta_{\mathbf{k}}(\tau)$ . The symmetry imposed on the modal coefficients produces  $\alpha_{\mathbf{k}}(\tau) = \alpha_{-\mathbf{k}}(\tau)$  and,  $\beta_{\mathbf{k}}(\tau) = -\beta_{-\mathbf{k}}(\tau)$ . Consequently, the modal coefficient  $\beta_{\mathbf{0}}(\tau)$  is zero. Taking into account the symmetries of the modal coefficients, and if  $N$  is the order of truncation, then there will be  $2N(N+1) + 1$  independent modal coefficients  $\alpha_{\mathbf{k}}$  and  $2N(N+1)$  independent  $\beta_{\mathbf{k}}$ . From equation (3) the equation of motion for the coefficient  $\alpha_{\mathbf{0}}(\tau)$  can be written as

$$\alpha_{\mathbf{0}}''(\tau) + \alpha_{\mathbf{0}}^3(\tau) + \mathcal{V}_{\mathbf{0}}(\alpha_{\mathbf{0}}, \alpha_{\mathbf{k}}, \beta_{\mathbf{k}}) = 0, \quad (4)$$

with the last term representing nonlinear mode–mode couplings.  $\alpha_{\mathbf{0}}(\tau)$  is identified as the homogeneous mode of the inflaton. Note that by neglecting the potential-like term  $\mathcal{V}_{\mathbf{0}}$ , namely considering the modal coefficients  $\alpha_{\mathbf{k}}$  and  $\beta_{\mathbf{k}}$  very small ( $\mathbf{k} \neq \mathbf{0}$ ), we come up with the equation that governs the evolution of the homogeneous component of the inflaton in a period after inflation when all other modes are still small in amplitude [2]. The exact solution in this situation is oscillatory, given in terms of an elliptic cosine with modulus  $\sqrt{2}$ , up to a rescale of the conformal time.

In general, for any other modal coefficient ( $\alpha_{\mathbf{k}}, \beta_{\mathbf{k}}$ ) and for any order of truncation, equation (3) yields

$$\begin{aligned} \alpha_{\mathbf{k}}''(\tau) + (\omega_{\mathbf{k}}^2 + 3\alpha_{\mathbf{0}}^2(\tau))\alpha_{\mathbf{k}}(\tau) + \mathcal{V}_{\mathbf{k}}(\alpha_{\mathbf{0}}, \alpha_{\mathbf{k}}, \beta_{\mathbf{k}}) &= 0 \\ \beta_{\mathbf{k}}''(\tau) + (\omega_{\mathbf{k}}^2 + 3\alpha_{\mathbf{0}}^2(\tau))\beta_{\mathbf{k}}(\tau) + \mathcal{U}_{\mathbf{k}}(\alpha_{\mathbf{0}}, \alpha_{\mathbf{k}}, \beta_{\mathbf{k}}) &= 0 \end{aligned} \quad (5)$$

where again  $\mathcal{V}_{\mathbf{k}}$  and  $\mathcal{U}_{\mathbf{k}}$  represents all types of nonlinear mode–mode couplings. The first two terms of both equations (5) above describe the linear regime for the modes  $\mathbf{k} \neq \mathbf{0}$ , namely when the amplitude of these modes are still small and we can neglect the nonlinear couplings  $\mathcal{V}_{\mathbf{k}}(\alpha_{\mathbf{0}}, \alpha_{\mathbf{k}}, \beta_{\mathbf{k}})$  and  $\mathcal{U}_{\mathbf{k}}(\alpha_{\mathbf{0}}, \alpha_{\mathbf{k}}, \beta_{\mathbf{k}})$ . In this situation  $\alpha_{\mathbf{0}}$  has an oscillatory behaviour as mentioned previously, and equations (5) assume the form of the Lamé equation, so that depending on a convenient choice of  $\omega_{\mathbf{k}}$ , dictated by the corresponding stability/instability chart, parametric resonance will occur [2]. The resonant modes will

lead the dynamics into the nonlinear regime, therefore restructuring the resonance through basically two concomitant mechanisms, backreaction on the homogeneous mode via the nonlinear couplings  $\mathcal{V}_0$ , and on the nonzero modes themselves (resonant and nonresonant) via  $\alpha_0$  and via the nonlinear couplings  $\mathcal{V}_k$  and  $\mathcal{U}_k$ . For instance, expansion of  $\mathcal{V}_0$  given in (4) yields  $\mathcal{V}_0 = 6 \sum_{\mathbf{k}} (\alpha_{\mathbf{k}}^2 + \beta_{\mathbf{k}}^2) \alpha_0 + \dots$ , where the first term may be interpreted, in a QFT manner, as connected to one-loop Hartree corrections which will begin to restructure the resonance (due to the backreaction of the created quanta of the inflaton on its homogeneous mode), and further terms may be interpreted as describing higher-order loop corrections.

The dynamical system contained in equations (4) and (5) is integrated with initial conditions taken according to the following considerations [3, 10]. The fluctuations in the inflaton are quantum in origin, and it is appropriate to consider the field to be in the vacuum state at the end of inflation. The zero mode (homogeneous mode) is semiclassical from the beginning. By virtue of our rescaling its initial value is  $\alpha_0(0) = 1$ , and we choose  $\alpha'_0(0) = 0$  as the definition of the moment  $\tau = 0$  when the oscillations of the inflaton start. From these initial conditions the time dependence of the homogeneous component of the inflaton will be obtained from equation (3), once the initial conditions for the nonzero modes  $\alpha_{\mathbf{k}}$  and  $\beta_{\mathbf{k}}$  are specified. The classical complex coefficients  $a_{\mathbf{k}}(\tau) = \alpha_{\mathbf{k}}(\tau) + i\beta_{\mathbf{k}}(\tau)$ , solutions of equation (3), can be interpreted as  $c$ -number amplitudes associated with processes of creation and annihilation of quantum fluctuations of the inflaton field in the mode  $\mathbf{k}$ . At the end of inflation, in the vacuum state, they may be given as

$$\begin{aligned} a_{\mathbf{k}}(0) &= \sqrt{\frac{\lambda}{2\Omega_{\mathbf{k}}}} |A_{\mathbf{k}}| e^{2\pi i r_{\mathbf{k}}}, \\ a'_{\mathbf{k}}(0) &= \left[ -i\Omega_{\mathbf{k}} + \frac{a'}{a}(0) \right] a_{\mathbf{k}}(0) \end{aligned} \tag{6}$$

where  $\Omega_{\mathbf{k}}^2 = \omega_{\mathbf{k}}^2 + 3\alpha_0(0)^2$ ,  $A_{\mathbf{k}}$  is a number randomly taken from a Gaussian distribution with zero mean and unit variance, and  $r_{\mathbf{k}}$  is a random number taken from the interval  $[0, 1]$ . We note that  $\lambda$  regulates the magnitude of initial quantum evolutions in nonzero modes relative to the magnitude of the zero mode; in our parametrization,  $(a'/a)(0) \approx 1$  and independent of  $\lambda$ . In obtaining equations (6), we treated the inflaton field as a free quantum field in the vacuum state at  $\tau = 0$ , with the  $c$ -number amplitude  $a_{\mathbf{k}}(\tau)$  satisfying the harmonic oscillator equation given by the linearized part of (3); also they are applicable in the adiabatic limit, namely  $\Omega'_{\mathbf{k}} \ll \Omega_{\mathbf{k}}^2$ . This choice of initial conditions is a good approximation when applied prior to the onset of resonance, but the assumptions leading to them are certainly violated at later times although we may consider that they fix the quantum nature of the fluctuations involved in later processes. A complete quantum-mechanical description of processes in the full nonlinear regime remains to be done. In order to proceed with the integration of equations (4), (5), we have set  $N = 2$  resulting in a dynamical system constituted by 25 independent second-order equations. Our guide for choosing a suitable value for  $L$  is the linearized regime described after neglecting the nonlinear mode-mode couplings  $\mathcal{V}_k$  and  $\mathcal{U}_k$  in equations (5). Several modes were selected which undergo an initial phase of parametric resonance by considering the stability/instability chart for the Lamé equation that governs the evolution of the modes  $\alpha_{\mathbf{k}}$  and  $\beta_{\mathbf{k}}$  in the linearized version [2]. We then set  $L = 5\pi/\sqrt{2}$  such that all modes with  $|l| = 2, |m| = 1$  are inside the instability band (in this case  $\omega_{|2||1|}^2 = 1.6$ ) and are amplified.

### 3. Numerical results

We have performed numerical experiments [12] with sets of initial conditions determined by different values of  $\lambda$  ranging from  $10^{-13}$  to  $10^{-4}$  that determines (cf equation (6)) the initial amplitude of the modes  $\alpha_{\mathbf{k}}$  and  $\beta_{\mathbf{k}}$ . As a consequence, the only observed physical feature due to the choice of distinct values of  $\lambda$  is the time required for the nonlinearities described by the potential terms  $\mathcal{V}_0$ ,  $\mathcal{V}_{\mathbf{k}}$  and  $\mathcal{U}_{\mathbf{k}}$  to become important. These nonlinear effects include the end of the initial stage of preheating with the suppression of the exponential growth of the resonant modes due to parametric resonance and the backreaction and rescattering followed by thermalization which is, as we shall see, associated to the onset of a turbulent regime.

In figure 1, the long-time behaviour of the homogeneous mode of the inflaton field,  $\alpha_0(\tau)$ , the resonant mode  $\beta_{12}(\tau)$  and the nonresonant mode  $\alpha_{11}(\tau)$  are depicted for  $\lambda = 10^{-4}$ . We have identified three distinct phases, where the particular duration of each phase is dictated by the value of  $\lambda$ . In the first phase that lasts from  $\tau = 0$  to  $\tau \approx 80$ ,  $\alpha_0(\tau)$  oscillates with constant amplitude indicating that the mode–mode couplings present in  $\mathcal{V}_0$  (cf equation (4)) have negligible influence. The behaviour of the resonant mode  $\beta_{12}(\tau)$  and the nonresonant mode  $\alpha_{11}(\tau)$  is in agreement with the prediction provided by the linearized theory, i.e. the former experiences exponential growth while the latter oscillates without changing its amplitude considerably.

At this point it will be useful to discuss briefly the influence of the truncation order  $N$  in the decay of the inflaton. By increasing  $N$  more modes are added in the decomposition (2), so increasing the number of independent equations. From the Galerkin decomposition it is expected that as  $N \rightarrow \infty$  the error between the exact and the approximate values of the inflaton approaches zero. On the other hand, according to an aforementioned aspect of the Galerkin method, a relatively small truncation is able to reproduce efficiently the basic skeleton of the dynamics of the problem under consideration. Indeed, this is confirmed by some numerical experiments in which the truncation order is increased from  $N = 2$  (48 equations) to  $N = 4$  (162 equations). In figure 2 the evolution of  $\alpha_0$  for  $N = 2, 3$  and 4 is depicted. It is then important to notice that the end of the first phase and the subsequent one are almost identical no matter what the chosen truncation order.

A quantitative measure of the sum of all modal fluctuations produced about the homogeneous mode is given by the variance  $\sigma^2 = \langle (\varphi - \alpha_0)^2 \rangle = \sum (\alpha_{\mathbf{k}}^2 + \beta_{\mathbf{k}}^2)$ , where  $\alpha_0$  is the expected value of the inflaton field. In the Galerkin projection method used, it is easy to compute the long-time behaviour of the variance and show that, during the initial phase, the variance grows as expected by the linear theory of preheating (cf figure 3). As we shall see, the power spectrum of the variance will be used to make a definite characterization of the final turbulent phase as a thermalization phase due to the onset of a turbulent regime.

In the second phase, lasting from  $\tau \approx 80$  to  $\tau \approx 240$ , the nonlinear mode–mode couplings start to alter the evolution of the homogeneous mode  $\alpha_0(\tau)$ , and of the resonant and nonresonant modes as well. Basically, this phase is characterized by the end of the parametric resonance, and therefore signals the beginning of the restructuring of the resonance. From figure 1, it can be seen that  $\alpha_0(\tau)$ , the resonant mode  $\beta_{12}(\tau)$  and the variance oscillate with modulated amplitude and the nonresonant mode  $\alpha_{11}(\tau)$  oscillates



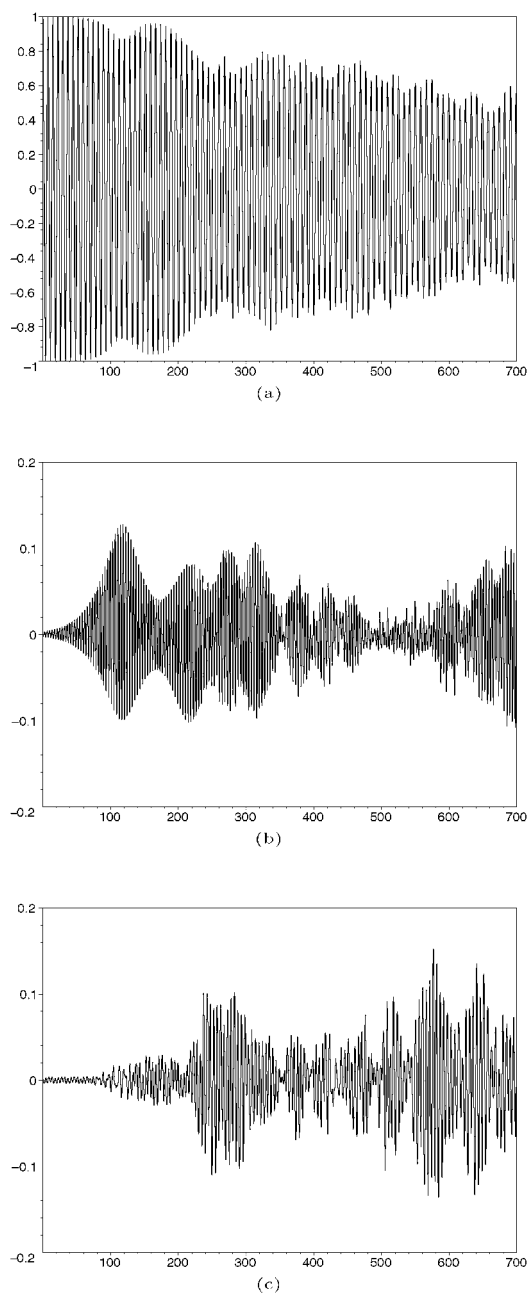


**Figure 1.** The behaviour of (a) the homogeneous mode  $\alpha_0(\tau)$ , (b) a typical resonant mode  $\beta_{12}(\tau)$  and (c) a nonresonant mode  $\alpha_{11}(\tau)$  for  $\lambda = 10^{-4}$ . The overall dynamics is characterized by three phases: the linearized phase from  $\tau = 0$  to  $\tau \approx 80$ , where the conventional preheating takes place; the *quasi-periodic* phase ( $\tau \approx 80$ – $240$ ), whose relevant feature is the end of the parametric resonance; and finally, the third phase—the *turbulent* phase. In this last phase there is no distinction between a resonant and a nonresonant mode due to the effective energy transfer from the inflaton to all modes.

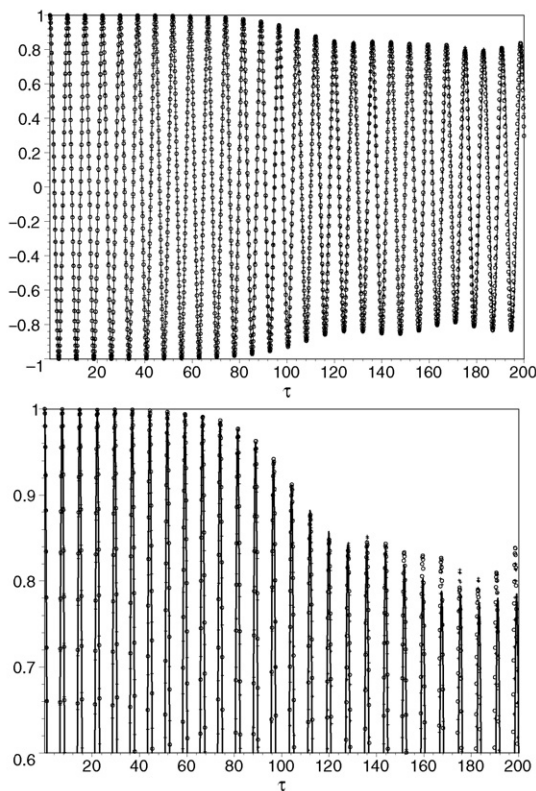


**Figure 2.** The evolution of the homogeneous mode  $\alpha_0(\tau)$  for  $N = 2$  (cross)  $N = 3$  (circle) and  $N = 4$  (solid) truncations. The figure at bottom is a snapshot of the upper envelope showing that its behaviour in the first phase and in the beginning of the subsequent one are almost identical, for the several truncation orders considered.

with increasing amplitude. Note that a minimum of the envelope of the oscillating mode  $\alpha_0(\tau)$  coincides approximately with a maximum of the envelope of the resonant mode  $\beta_{12}(\tau)$ , and vice versa, indicating a process of rescattering between these modes. Indeed, these nonlinear effects constitute the first manifestations of what is known as backreaction and rescattering, which in our dynamical system approach are entirely contained in the potential terms  $\mathcal{V}_0$ ,  $\mathcal{V}_k$  and  $\mathcal{U}_k$ . Then, we may denote this phase as the *quasi-periodic* phase.

#### 4. The turbulent regime

The third phase initiates at  $\tau \approx 240$  when the amplitude of the homogeneous mode reaches a minimum of approximately 70% of its initial value. Remarkably, this feature was found for all values of  $\lambda$  in our numerical experiments. As can be seen from figure 1, the homogeneous mode oscillates in an irregular pattern of modulated amplitude followed by a sequence of small bursts. Nonetheless, the most important aspect to be pointed out is the continuous decay of  $\alpha_0(\tau)$ . It is no longer possible to make a distinction between the resonant and nonresonant modes. The variance displays a completely chaotic



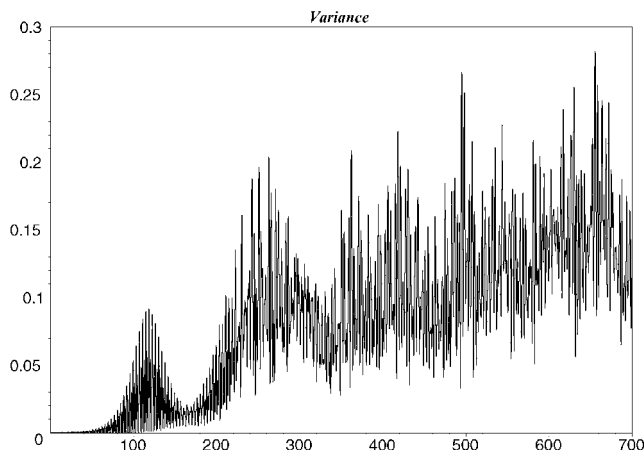


**Figure 3.** Behaviour of the variance.

pattern. These features are a dramatic consequence of the action of nonlinearities, namely the backreaction of the created particles into the homogeneous mode, as well as the rescattering of the produced particles into all other modes. Eventually, there will be no distinction whatsoever between the homogeneous mode and any other mode. Physically, this means that all modes will be on average equally populated, the particles dynamically transferring and distributing the energy among the modes, producing, in this way, the thermalization. Indeed, figure 4 depicts a sequence of the power spectra of the variance evaluated at several times, from the first to the third phase. This transition is constituted by period bifurcations, giving rise to approximate frequencies  $\frac{1}{3}\omega_1$ ,  $\frac{1}{2}\omega_1$ ,  $\frac{5}{7}\omega_2$  and  $\frac{5}{8}\omega_2$ , with  $\omega_1 \simeq 1.77$  and  $\omega_2 \simeq 3.45$ , characteristic of a typical road to turbulence [13]. From the power spectrum for  $\tau = 655.36$ , the presence of broad band portions can be noted, despite the presence of sharp frequencies, which tend to disappear asymptotically. This last phase is denoted as the *turbulent* phase. It is worth mentioning that the exact moment of onset of chaos may depend on the truncation order due to the distinct number of modes to be excited. Nevertheless, the presence of these three phases seems to be robust and independent of the truncation order. A comment is in order here. Our characterization of the onset of chaos was qualitatively given by the presence of a broad band portion of the power spectrum of the variance analogous to the analysis of [3]; on the other hand, a quantitative characterization was tested in [4] with the use of Lyapunov exponents associated with the phase space dynamics of the scalar field. Both results indicate that the onset of the chaotic regime occurs at the end of preheating.

Another relevant feature of this turbulent phase can be displayed by examining the distribution of energy as a function of modal wavenumber, characterizing the energy distribution per scale and making explicit the dynamical transfer of energy across the spectrum towards higher wavenumbers (small scales). Within our formulation, the energy  $E_\phi = \lambda\sqrt{-g}\rho_\phi$  expressed in the dimensionless variables is decomposed according to (2) as  $E_\phi = \sum_{\mathbf{k}} E_{\mathbf{k}}(\tau)\psi_{\mathbf{k}}$ . For large values of  $\tau$ , corresponding to the turbulent phase,  $E_{\mathbf{k}}$  is given by

$$E_{\mathbf{k}} \simeq \sum_{\mathbf{n}} \left( \frac{1}{2} a'_{\mathbf{n}} a'_{\mathbf{k}-\mathbf{n}} + \frac{2\pi^2}{L^2} \mathbf{n} \cdot (\mathbf{n} - \mathbf{k}) a_{\mathbf{n}} a_{\mathbf{n}-\mathbf{k}} \right) + \sum_{\mathbf{m}} \sum_{\mathbf{l}} \sum_{\mathbf{k}} \frac{1}{4} a_{\mathbf{n}} a_{\mathbf{l}} a_{\mathbf{m}} a_{\mathbf{k}-\mathbf{n}-\mathbf{l}-\mathbf{m}}. \quad (7)$$

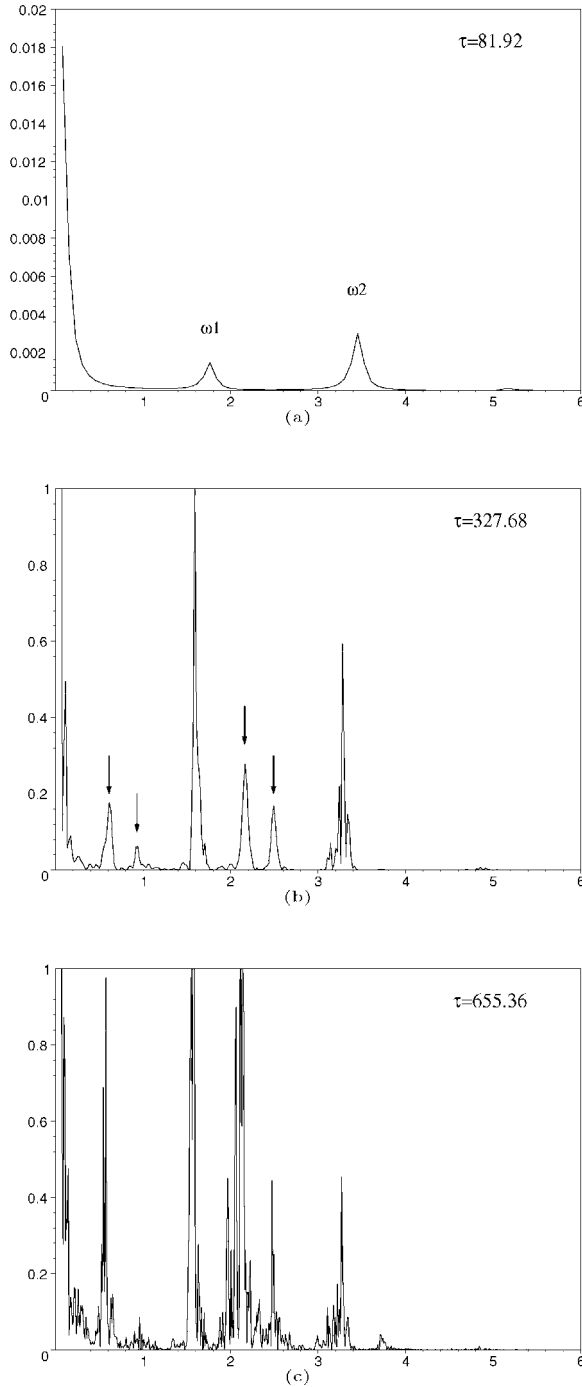


**Figure 4.** Power spectra of the variance evaluated at  $\tau = 81.92$ ,  $\tau = 327.68$  and  $\tau = 655.36$ , the last two corresponding to the third phase. It is worth observing that this sequence shows the periodic bifurcations  $\frac{1}{3}\omega_1$ ,  $\frac{1}{2}\omega_1$ , for the first peak  $\frac{5}{7}\omega_2$ , and  $\frac{5}{8}\omega_2$ , for the second. This behaviour is typical of the onset of turbulence found in fluid mechanics, as for instance in Couette flow.

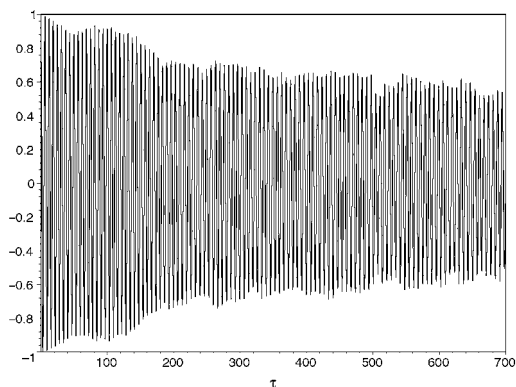


**Figure 5.** Decay of the homogeneous mode in the case of a three dimensional spatial domain.

Here our numerical calculations were performed in three dimensions, so that in the above expression  $\mathbf{k} = (l, m, n)$ . This generalization naturally encompasses more modes in the Galerkin decomposition (2) than in the two dimensional case, which provides a direct test for the convergence of this decomposition, along with a more realistic treatment of the problem. Before considering the energy spectrum, and for the sake of completeness, we depict the plot of the homogeneous mode in figure 5. As can be seen, this graph is qualitatively identical to the corresponding one of figure 1(a), indicating that the main features of the dynamics are not altered by considering the three dimensional case. Indeed, the smoothness of the decay of the homogeneous mode due to the presence of more modes, and therefore a better approach to the continuum limit, should be noticed.

In figure 6(a) we exhibit the spectrum of the energy  $\mathcal{E}_k$  in wavenumbers  $k$ , where the energy  $\mathcal{E}_k$  is the arithmetic average of all the energies  $E_{\mathbf{k}}$  whose corresponding  $\mathbf{k}$  have modulus  $k$ . The spectrum was evaluated at  $\tau = 2000$ , when the dynamics is in the turbulent phase. In order to have better statistics of points, we extended the Galerkin projection method to a truncation  $N = 2$ . The spectrum exhibits two distinct decoupled components separated by a gap of energy (cf figure 6). The majority of points lie in the second component connected to the energy distribution in large wavenumbers, or equivalently in small scales. This second piece of the spectrum can be understood as a consequence of the transfer of energy, initially stored in the homogeneous mode, to small scale modes. It can be interpreted as corresponding to a thermalized part of the system in the so-called inertial range of turbulent regimes, characteristic of statistical equilibrium at large wavenumbers. Indeed, such a component of the spectrum is fitted by the distribution law

$$\mathcal{E}_k = \mathcal{E}_0 \exp(-bk^2), \quad (8)$$

with the constants  $\mathcal{E}_0 = 0.0093$  and  $b = 0.0621$  obtained from the best fit depicted by the continuous line in figure 6(b). The distribution law (8) has the form of a Maxwell–Boltzmann distribution, which reinforces the interpretation that this turbulent component in the inertial range indeed corresponds to a thermalized part of the system. The thermalization is then seem to be a consequence of the complete chaotic dynamics of the strongly nonlinear coupled oscillators. In order to extract the value of the

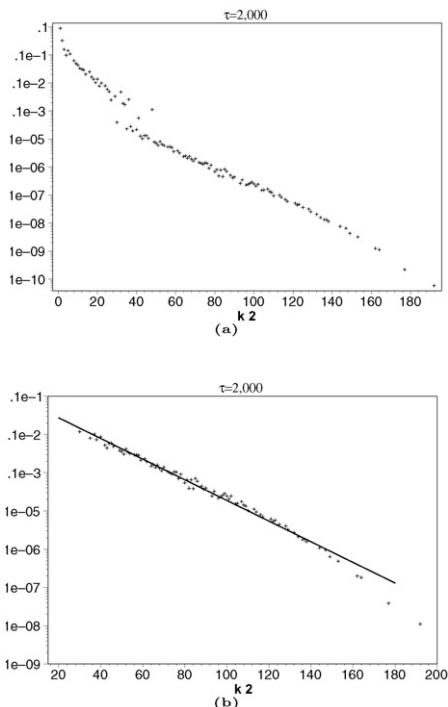


**Figure 6.** The energy spectrum  $\mathcal{E}_k$  evaluated at  $\tau = 2000$  when the dynamics is in the full turbulent regime. (a) The behaviour of  $\ln(\mathcal{E}_k/k^2)$  versus  $k^2$ . (b) The plot of  $\ln(\mathcal{E}_k/k^2)$  versus  $k^2$  for the points of the second component of the spectrum connected to the distribution of energy at large wavenumbers. The continuous straight line is the best fit of the Maxwell–Boltzmann distribution (8) with  $\mathcal{E}_0 = 0.0093$  and  $b = 0.0621$ .

temperature associated with such a thermal distribution we proceed as follows. Due to the reparametrization of our equations, the coordinates  $\mathbf{x}$  and the momenta  $\mathbf{k}$  were made dimensionless. Returning to the physical variables the argument of the exponential in the Maxwell–Boltzmann law is now expressed as

$$\frac{bL^2}{\lambda\phi_0^2 a_0^2} k_{\text{phys}}^2 \quad (9)$$

where  $L$  is the dimensionless characteristic length of the box,  $\phi_0$  and  $a_0$  are the values of the inflaton field and the scale factor at the beginning of preheating, respectively. In natural units ( $\hbar = c = k_B = 1$ ), the temperature of the thermalized component at  $\tau = 2000$  and corresponding to the small scales is given by

$$T_R = \frac{\lambda\phi_0}{b} \approx 10^2 \lambda M_{\text{Pl}} \approx 10^{17} \text{ GeV} \quad (10)$$

where  $b \simeq 0.0621$  is fixed by the fitting; also we have set  $a_0^2 = L^2$ ,  $\phi_0 \sim 3M_{\text{Pl}}$  and  $\lambda \sim 10^{-4}$  (the value adopted in our computation). It is interesting to note that this temperature is compatible with a reheating temperature. If a more realistic value of  $\lambda$  of the order of  $10^{-14}$  were adopted a much longer time evolution would be needed in order to achieve the turbulent regime. Possibly, in this situation  $b$  would be smaller in such a way as to

produce a compatible reheating temperature. This latter point deserves a more complete examination along with the calculation of a saturation value of  $b$  in a time when the homogeneous mode is energetically indistinguishable from other modes.

## 5. Conclusions

In conclusion, we gave an extended dynamical picture of the nonlinear decay of the inflaton with potential  $V(\phi) = \frac{1}{4}\lambda\phi^4$ , from the initial linear parametric resonance phase towards a final turbulent regime. We used the Galerkin projection method that describes the dynamics of the inflaton as a countable set of nonlinear coupled harmonic oscillators. The process develops in three distinct phases<sup>3</sup>, starting from the linear regime of parametric resonance to a final thermalization process due to the onset of turbulence in the dynamics. An essential feature of the process is the transition from the quasi-periodic phase, in which the parametric resonance is suppressed, towards a turbulent regime characterized by a highly effective transfer of energy among the homogeneous mode to all other modes, due to the nonlinear coupling of the modes that dominates the dynamics in the long term. As a result, the state of thermalization is accomplished due to the development of a full turbulent phase. The onset of turbulence is characterized through the frequency spectrum of the variance (a measure of the sum of all fluctuations about the homogeneous mode). This spectrum is evaluated at several times, from the first to the third phase, clearly showing period doubling towards a broad band spectrum characteristic of a full turbulent regime. Two features of the turbulent stage are displayed: first, an effective mechanism of transfer of energy among the homogeneous modes and all other modes, initially resonant or not; second, the distribution of energy versus the modal wavenumber, characterizing the energy distribution per scale, which shows two distinct decoupled components. One of the components, connected to the energy distribution in small scales, has a Maxwell–Boltzmann form, characteristic of the statistical equilibrium at large wavenumbers in the inertial range of the turbulent regime. In this situation we found that the equilibrium temperature is  $T_R \simeq \lambda\phi_0 b^{-1} \approx 10^2 \lambda M_{\text{Pl}}$ , for  $b \simeq 0.0621$  for  $\tau = 2000$ .

We finally remark that Micha and Tkachev [14] have recently discussed the process of thermalization in the final stages of reheating in a  $\lambda\phi^4$  inflationary model. Their computation suggests that the evolution of particle spectra is self-similar at the final turbulent stages. Based on this result they make an ansatz of the evolution of the occupation number spectra and, by assuming a kinetic theory description, they evaluate the temperature at thermalization to be  $T \sim \lambda^2 M_{\text{Pl}}$ . In our approach, the Galerkin projection method allowed us to extend the evolution of the amplitudes  $a_{\mathbf{k}}$  up to a phase where a turbulent regime is clearly established, and the numerical evaluation of the energy distribution per modal wavenumber shows a thermalized component that has a Maxwell–Boltzmann distribution with temperature  $T \simeq 10^2 \lambda M_{\text{Pl}}$ . Although our calculations use fluctuations of the inflaton field that from the start have a quantum nature, the explanation of this large discrepancy between our result and that of reference [14] can only be fixed when a complete quantum-mechanical description of the full nonlinear regime of the field is available.

<sup>3</sup> It is important to remark that the presence of these three phases is robust with respect to the change of  $L$ , only the timescales for each phase are modified.

## Acknowledgments

The authors acknowledge the financial support of CNPq. HPO is grateful to ICTP where part of the present work was undertaken. We would like to thank Dr da Mota for helping us with some routines using Maple, and Dr Skea for the routines in C++.

## References

- [1] Kofman L, Linde A and Starobinsky A A, 1994 *Phys. Rev. Lett.* **73** 3195 [SPIRES]
- [2] Patrick Greene B, Kofman L, Linde A and Starobinsky A A, 1997 *Phys. Rev. D* **56** 6175 [SPIRES]
- [3] Khlebnikov S Yu and Tkachev I I, 1996 *Phys. Rev. Lett.* **77** 219 [SPIRES]  
Prokopec T and Ross T G, 1997 *Phys. Rev. D* **55** 3768 [SPIRES]
- [4] Felder G and Kofman L, 2001 *Phys. Rev. D* **63** 103503 [SPIRES]
- [5] Kaiser D, 1996 *Phys. Rev. D* **53** 1776 [SPIRES]  
Kaiser D, 1997 *Phys. Rev. D* **56** 706 [SPIRES]  
Boyanovsky D, Cormier D, Vega H J, Holman R and Kumar S P, 1998 *Phys. Rev. D* **57** 2166 [SPIRES]
- [6] Holmes P, Lumley J L and Berkooz G, 1998 *Turbulence, Coherent Structures, Dynamical Systems and Symmetry* (Cambridge: Cambridge University Press)
- [7] Kodama H and Hamazachi T, 1996 *Prog. Theor. Phys.* **96** 949 [SPIRES]  
Hamazachi T and Kodama H, 1996 *Prog. Theor. Phys.* **96** 1123 [SPIRES]
- [8] Basset B, Kaiser D and Maartens R, 1999 *Phys. Lett. B* **455** 84 [SPIRES]  
Basset B, Tamburini F, Kaiser D and Maartens R, 1999 *Nucl. Phys. B* **561** 188 [SPIRES]
- [9] Finelli F and Brandenberger R, 1999 *Phys. Rev. Lett.* **82** 1362 [SPIRES]
- [10] Easther R and Parry M, 2000 *Phys. Rev. D* **62** 103503 [SPIRES]
- [11] Turner M S, 1983 *Phys. Rev. D* **28** 1243 [SPIRES]
- [12] Aguirregabiria J M, *Dynamic solver*, <http://tp.lc.ehu.es/jma.html>
- [13] Swinney H L and Gollub J P (ed), 1985 *Hydrodynamics Instabilities and the Transition to Turbulence* 2nd edn (New York: Springer)
- [14] Micha R and Tkachev I, 2003 *Phys. Rev. Lett.* **90** 121301 [SPIRES]